

# Investigation of Symmetrical Optimum PI Controller based on Plant and Feedback Linearization in Grid-Tie Inverter Systems

Iwan Setiawan\*<sup>‡</sup>, Mochammad Facta\*, Ardyono Priyadi\*\*, Mauridhi Hery Purnomo\*\*

\*Department of Electrical Engineering, Universitas Diponegoro (Undip), Semarang 50275 Indonesia.

\*\* Department of Electrical Engineering, Institut Teknologi Sepuluh Nopember, Surabaya 60111 Indonesia.

(iwansetiawan@live.undip.ac.id, mochfacta@gmail.com, priyadi@ee.its.ac.id, hery@ee.its.ac.id)

‡ Corresponding Author: Iwan Setiawan, Kampus Teknik Elektro Undip Tembalang Semarang, Indonesia, Tel: +62 24 7460057, Fax: +62 24 7460057, iwansetiawan@live.undip.ac.id

Received: 27.01.2017 Accepted: 22.02.2017

**Abstract-** Up to now, conventional proportional-integral (PI) controllers are the most common DC-bus voltage regulation strategy used in grid-tie inverter systems. The popularity of PI controllers are mainly due to the simplicity of its control structure and the feasibility of its control performance. The main aim of this work is to investigate and to compare the performance of two linearization techniques in which PI controller implemented to handle the nonlinear problem of the DC-bus voltage regulation, namely: plant linearization and feedback linearization technique. To get optimum responses, in this paper, the PI controller parameters were chosen by the popular symmetrical optimum tuning method. By using simulation study under Matlab/Simulink software environment, it is shown that both the linearization techniques based PI controller have almost the same performance in response to relatively small power disturbances. Whereas for the relatively large power disturbances, the performance of the plant linearization based-PI controller, although not too significant, is more superior than that based on the feedback linearization technique.

**Keywords** DC bus; feedback linearization, grid-tie inverter, plant linearization, symmetrical optimum tuning method.

## Nomenclature

$V$	Inverter voltage magnitude (V)
$E$	grid voltage magnitude (V)
$\delta$	phase angle difference (rad)
$L$	Line inductance (H)
$R$	Line resistance (ohm)
$C$	DC bus capacitance (F)
$\omega_g$	Grid frequency
$\omega_s$	Synchronous frequency
$V_{dc}$	DC bus voltage
$i_d, i_q$	d-axis component of grid voltage and current vector
$v_d, v_q$	direct and quadrature component of the inverter voltage vector
$e_d, e_q$	direct and quadrature component of the grid voltage vector
$u_{PI}$	output of the PI controller
$K_p$	Proportional gain

$T_i$	Time integral
$T_{cl}$	desired time constant of closed loop system
$P_g$	active grid power
$Q_g$	reactive grid power
$i_{dc_s}$	Renewable power source DC current
$i_{dc_g}$	Grid side converter DC current

## 1. Introduction

Grid-tie inverters recently play important role in many grid-connected power system applications including doubly fed induction generator based wind turbine [1-3], on-grid photovoltaic systems [4-5], Active Power Filter/STATCOM [6-8], high voltage direct current (HVDC) transmission systems [9-10], active rectifiers [11], and Dynamic Voltage Restorer [12].

In the on-grid power system applications, the main responsibility of the inverters and their associated controller

basically are to deliver both active and/or reactive power from utilities to the grid or vice versa.

In the vector control method, the magnitude and direction of the active power flow generally controlled indirectly by regulating the DC bus capacitor voltage at a certain level, whereas the reactive power is controlled by manipulating the quadrature component of the current vector directly.

Based on the power balance theorem, the DC bus voltage dynamic in the grid-tie inverter systems basically is governed by a nonlinear differential equation. However due to the design and implementation simplicity, up to now, the most common strategy used to regulate the DC bus capacitor voltage is a linear PI control method.

Technically, there are two general linearization approaches that could be chosen to regulate the nonlinear dynamic of the DC bus voltage by using the linear PI controller: (1) Plant linearization technique such as used by Pena et.al [13] and Abad et.al [14] and (2) Feedback linearization technique such as used by Song et.al [15] and Setiawan et.al [16]. Although the implementation of these two methods could be found in many works, to the best of author’s knowledge, none of the papers try to investigate and compare the control performance resulted by these two methods.

The main objectives of this paper are two folds: (1) To design the PI controller for regulating DC bus capacitor voltage in the on-grid renewable power generation systems by using the plant linearization and feedback linearization methods, (2) to analysis and compare the transient performance achieved by those different feedback control scheme. To get the optimum performance, in this work, the PI control parameter for both methods are tuned by using relatively popular method that well known as symmetrical optimum tuning method [17].

The remainder of the paper is organized as follows. Section 2 describes respectively the model of the on-grid renewable power generation system and the symmetrical optimum PI tuning method. In Section 3, the design of the DC bus capacitor voltage regulator in the on-grid renewable power generation system by using the plant and feedback linearization methods will be discussed, next, Section 4 present the simulation results and discuss the transient performance of the control system. Finally, the conclusions are drawn at Section 5.

**2. System Models**

*2.1. Current dynamics and Power Transfer of Grid-Tie Inverter Model*

Fig.1 shows a general topology of the grid-tie inverter in on-grid renewable power generation system that is used in this investigation. By ignoring the cable resistance, In the steady state, the grid active (P) and reactive power (Q) could be simply represented by (1) and (2).

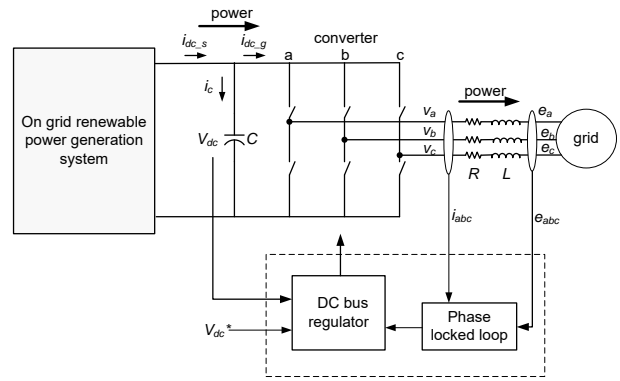


**Fig.1.** a grid-tie inverter in the on-grid renewable power generation system

$$P_g = \frac{VE\sin(\delta)}{\omega_s L} \tag{1}$$

$$Q_g = \frac{V}{\omega_s L}(V\cos(\delta) - E) \tag{2}$$

Based on the above two equations, it is clear that for the certain grid voltage, the active and reactive grid power respectively could be controlled directly by manipulating the phase and magnitude of the inverter output voltage.

By using the Clark and Park transformations, the grid-tie inverter circuit model of Fig.1 could be represented in the *d-q* circuit model as shown at Fig.2. In the *d-q* circuit model, the sinusoidal current and voltage of the grid and inverter systems will be appear as dc variables that relatively easy to be manipulated. By refer to Fig. 2, the current dynamic of the grid-tie inverter system could be represented as shown at (3) and (4).

$$\frac{di_d}{dt} = -\frac{R}{L}i_d + \frac{1}{L}v_d + \frac{1}{L}(-e_d + \omega_s Li_q) \tag{3}$$

$$\frac{di_q}{dt} = -\frac{R}{L}i_q + \frac{1}{L}v_q + \frac{1}{L}(-e_q - \omega_s Li_d) \tag{4}$$

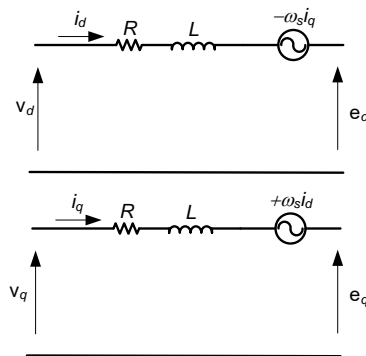


**Fig. 2.** *d-q* circuit model of the grid-tie inverter system

From (3) and (4), it is clear that the dynamic of the *d-q* grid current vector components basically could be controlled independently by manipulating the *d-q* voltage components of the inverter output. If the inverter output are chosen as shown in (5) and (6).

$$v_d = u_{PI} + (e_d - \omega_s Li_q) \tag{5}$$

$$v_q = u_{PI} + (e_q + \omega_s Li_d) \tag{6}$$

Where

$$u_{PI} = K_p(1 + \frac{1}{T_i s})(I^*(s) - I(s)) \tag{7}$$

if  $K_p$  and  $T_i$  are determined by using the pole placement technique as shown in (8) and (9) below:

$$K_p = L/T_{cl} \tag{8}$$

$$T_i = L/R; K_i = K_p/T_i \tag{9}$$

then the closed loop transfer function of the grid  $d$ - $q$  current components now could be simplified as the first order system as shown at (10) [18].

$$\frac{I_d(s)}{I_d^*(s)} = \frac{I_q(s)}{I_q^*(s)} = \frac{1}{T_{cl}s+1} \tag{10}$$

Fig.3 shows the block diagram of the PI control system of the grid current vector components.

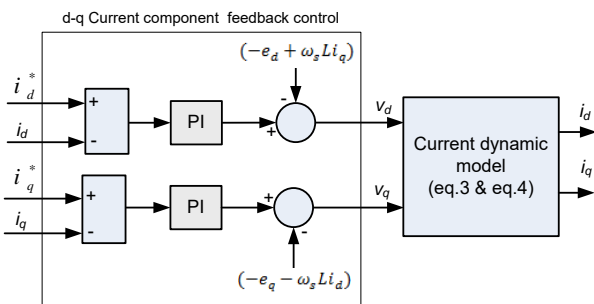


**Fig. 3.** Block diagram of the PI control system of the grid current components

If the grid voltage vector in the current dynamic model is chosen as the synchronously rotating frame of reference, then the active and reactive grid power could be calculated respectively by using (11) and (12).

$$P_g = \frac{3}{2}(e_d i_d) \tag{11}$$

$$Q_g = \frac{3}{2}(-e_d i_q) \tag{12}$$

**2.2. Symmetrical Optimum PI Tuning Method**

Historically, the Symmetrical Optimum (S.O) tuning method first proposed by Kessler in 1958. According to the S.O criteria, the parameters of the PI controller for the plant model shown in (13) could be determined by using (14) and (15).

$$H_{OL}(s) = \frac{K}{T_s(T_{eq}s+1)} \tag{13}$$

$$K_p = \frac{T}{aKT_{eq}} \tag{14}$$

$$T_i = a^2 T_{eq} \tag{15}$$

Where  $a$  is a parameter that determine the phase margin and damping ratio of the closed loop transfer function: The higher value of  $a$  will tend to increase both of the phase margin and damping ratio. For the detail explanation of the S.O tuning method, the readers are suggested to refer [19].

**3. Design of the DC Bus Voltage Regulator**

By refer to Fig.1, the dynamic of the DC bus capacitor voltage could be written as shown in (16)

$$\frac{v_{dc}}{dt} = -\frac{1}{C} i_{dc.g} + \frac{1}{C} i_{dc.s} \tag{16}$$

By considering the power balance theorem below:

$$v_{dc} i_{dc.g} = \frac{3}{2} e_d i_d \tag{17}$$

Then the dynamic of the DC bus capacitor voltage will be appeared as a non-linear differential equation as shown in (18):

$$\frac{v_{dc}}{dt} = -\frac{3}{2C} \frac{e_d}{v_d} i_d + \frac{1}{C} i_{dc.s} \tag{18}$$

**3.1. Design of the PI controller by using plant linearization Technique**

At around operating point, the non-linear dynamic of the DC bus voltage could be linearized as shown at (19).

$$\frac{v_{dc}}{dt} = -\frac{3e_d}{2Cv_{dc}^*} i_d + \frac{1}{C} i_{dc.s} \tag{19}$$

By substituting the  $d$ -axis grid current component from (10) into (19), the DC bus voltage dynamic now could be represented as shown in (20).

$$V_{dc}(s) = -\frac{3e_d}{2CV_{dc}^*} \frac{1}{(T_{cl}s+1)} i_d^*(s) + \frac{1}{C_s} i_{dc.s}(s) \tag{20}$$

By careful inspection, the dynamic of the DC bus voltage due to the  $I_d$  reference changes in (20) basically is equivalent with (13). Using the S.O method, the PI control parameters could be found easily as shown in (21) below.

$$K_p = \frac{2CV_{dc}^*}{3ae_d T_{cl}}; T_i = a^2 T_{cl}; K_i = \frac{K_p}{T_i} \tag{21}$$

Fig.4 shows the simplified PI control block diagram of the DC bus voltage based on plant linearization technique.

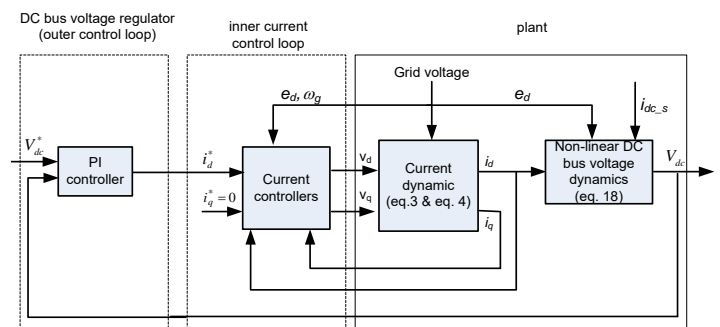


**Fig. 4.** Block diagram of the DC bus voltage control system based on plant linearization

**3.2. Design of the PI Controller by using Feedback Linearization Technique**

By refer to relations (10) and (18), the DC bus voltage dynamic mathematically could be directly represented as a linear feedback system as as shown in (22) below:

$$\frac{v_{dc}}{dt} = -\frac{3e_d}{2Cs} \frac{1}{(T_{cl}s+1)} u(s) + \frac{1}{C} i_{dc\_s} \quad (22)$$

Where

$$u(s) = \left( \frac{i_d^*(s)}{v_{dc}} \right) \quad (23)$$

From (23) it is clear that in the feedback linearization technique, the *d*-axis current component reference basically is the nonlinear signal that depend on both the PI controller output and the actual DC bus voltage. So by using S.O. method, the PI control parameters could be found easily by (24) below

$$K_p = \frac{2C}{3ae_d T_{cl}}; T_i = a^2 T_{cl}; K_i = \frac{K_p}{T_i} \quad (24)$$

Fig.5 shows the simplified DC bus voltage control system block diagram based on the feedback linearization.

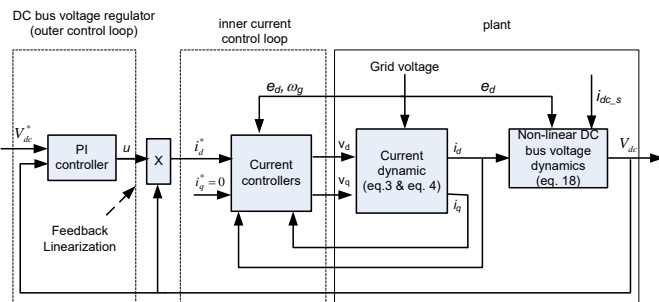


Fig.5. Block diagram of the DC bus voltage control system based on feedback linearization

4. Simulation Results and Discussion

Fig.6 shows the relatively complete block diagram of the grid-tie inverter in the on-grid renewable power generation systems that investigated in this study.

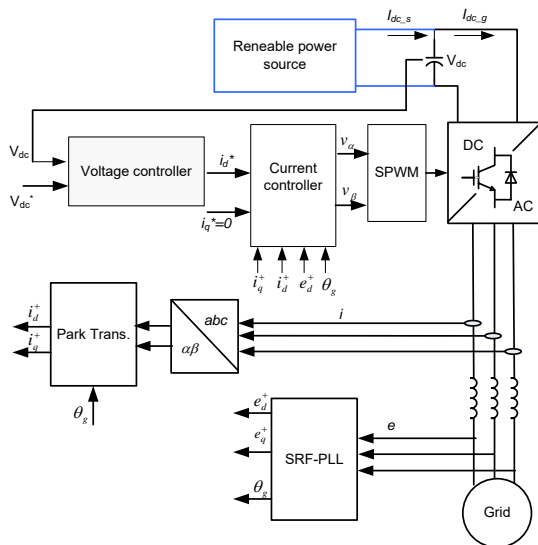


Fig.6. Simulation block diagram of the DC bus voltage control system in grid-tie inverter system

By using the grid-tie inverter system parameters as shown at Table 1, the PI control parameter for the inner current loop and the DC bus outer loop could be calculated as shown respectively in Table 2 and Table 3.

In this works, the phase angle and the magnitude of the grid voltage are estimated by using synchronous reference frame phase locked loop (SRF-PLL), whereas the renewable power generation system in the simulation block is emulated by using the controlled current source.

Table 1. The grid-tie inverter system Parameters

Parameter	value
$v_{LL}(V)$	310
$f(Hz)$	50
$R(ohm)$	0.02
$L(H)$	0.01
$C(uF)$	1200
$V_{dc}^*(V)$	650

Table 2. The PI control parameters for the inner current loop

Parameter	Value	Method
$K_p$	10	Pole placement $T_{cl}=0.001$ s
$K_i$	20	

Table 3. The symmetrical optimum PI control parameters with  $a=2$

Linearization Method	$K_p$	$K_i$
Plant Linearization	0.838	209.5
Feedback Linearization	0.00129	0.3225

4.1. The Current Loop Control Performance

Due to the performance of the inner current loop influence the performance of the DC bus voltage regulation directly. In this subsection, the performance of the inner current loop control will be investigated first.

By considering the current dynamic at the grid-tie inverter system is much faster compared to the DC bus voltage dynamic, than the desired closed loop time constant could be set as small as possible. However by considering the constraint of the current sampling rate, in this works, the desired closed loop time constant of the inner current loop is set 0.001s. Fig.7 shows the transient responses of the current and grid power to the change of the current reference.

From Fig. 7(a), it could be seen that for the step reference change of the  $i_d$  current vector component, the output can follow the reference almost instantly with the time constant about 0.001 second agree with the desired time. For the  $d$ - $q$  current vector components profile depicted in those plots, the actual three phase grid current and the grid power respectively are shown in Fig.7(b) and Fig.7(c).

4.2. The DC Bus Voltage Regulation Performance

In this subsection, the PI control performance of the DC bus voltage regulation based on the two linearization techniques are be discussed

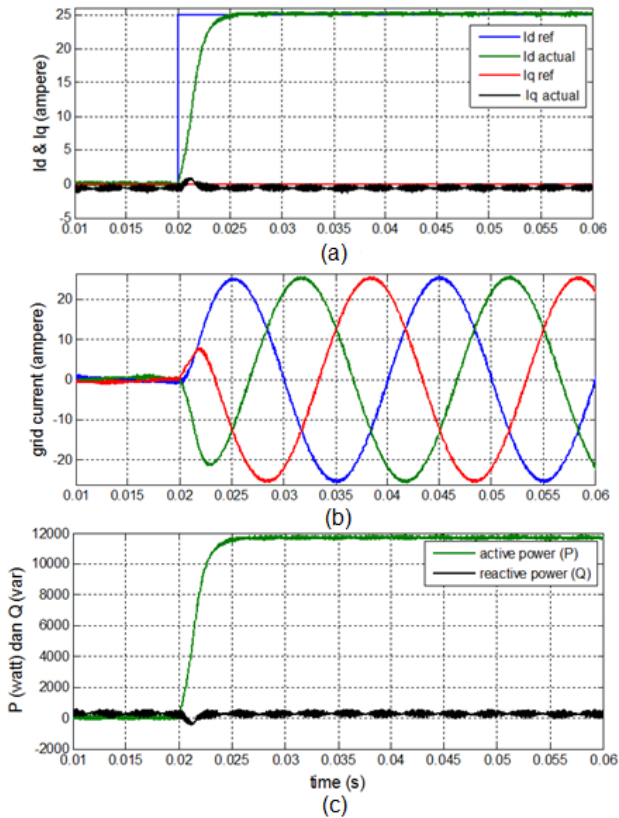


**Fig.7.** Transien Responses: (a) the *d-q* current vector component (b) the three phase grid current (c) the grid power

To investigate the control performance of DC bus voltage regulation, in this study, the DC bus voltage in the steady state will be disturbed by the sudden change of the power generated by source with different magnitude.

Fig.8 and Fig.9 respectively show the transient response of the DC bus voltage and the active grid power of feedback control system caused by the sudden changes of the power source with relatively small magnitude.

From the plots of Fig. 8(a) and Fig. 9(a), it could be seen that the transient response and the integral of time-weighted absolute error (ITAE) performance index of the plant linearization and the feedback linearization based PI controller system are almost the same: For the sudden power change of 2000 (5000) Watt in the renewable energy source, it is observed that the DC bus voltage will deviate from the steady state and rise with overshoot of 4.5 (10.75) volt. From the same plots it also could be seen that the settling time resulted by the different PI control scheme are about 0.01 second.

Whereas from the plots of Fig. 8(b) and Fig. 9(b), ones can see the transient response of the active grid power due to the relatively small sudden power change. From the plots it could be observed that the transient response resulted from the different PI control scheme are almost the same.

For the relatively large power disturbances, the transient response of the DC bus voltage and the active grid power respectively are shown in Fig.10 and Fig.11.

From the Fig. 10(a) and Fig. 11(a), it is shown that the dynamic of the DC bus voltage and the power of two PI control scheme are relatively difference. In this case, the

transient response of the PI control loop based on plant linearization have better performance than that based on the feedback linearization. For the sudden power change of 22 (23) KW, the DC bus voltage of the PI control loop based on plant linearization will be experiencing overshoot 65 volt with settling time about 0.025 second, whereas for the PI control loop based on feedback linearization, the DC bus voltage will be experiencing overshoot 70 volt with settling time about 0.03 second.

From the plots of Fig. 10(b) and Fig. 11(b), ones can observe the transient response of the active grid power due to the relatively large sudden power change.

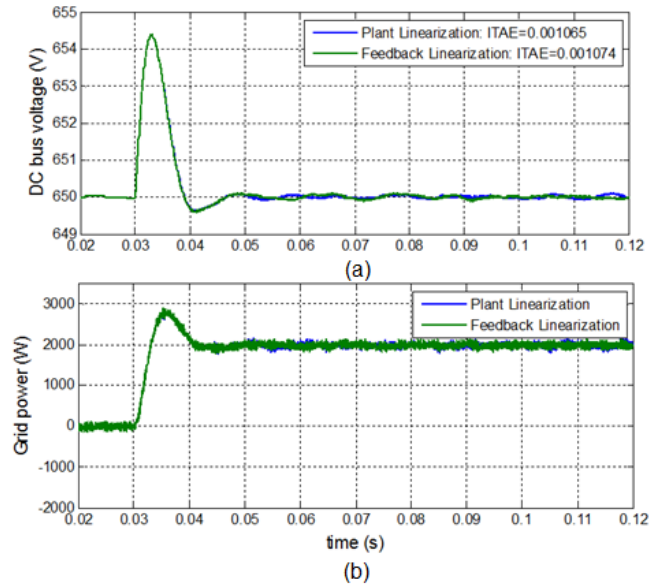


**Fig.8.** Transien Response of the small disturbance (2000W power change): (a) the DC bus voltage (b) the active grid power

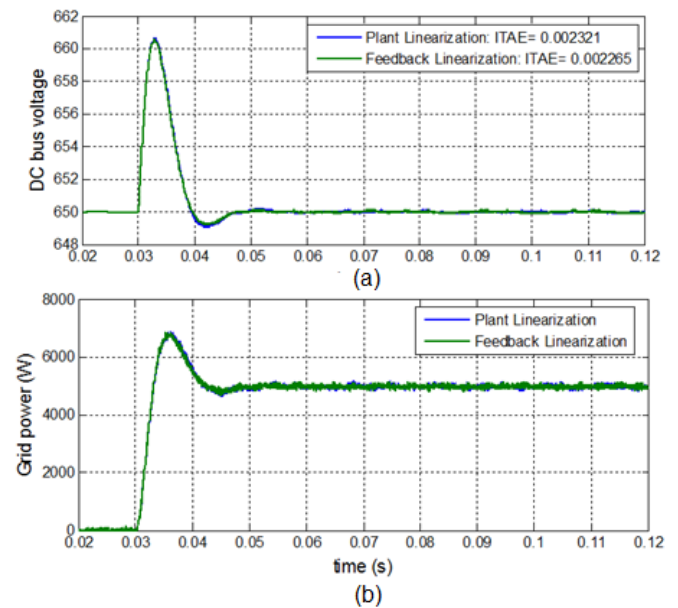


**Fig.9.** Transien Responses of the the small disturbance (5000W power change): (a) the DC bus voltage (b) the active grid power

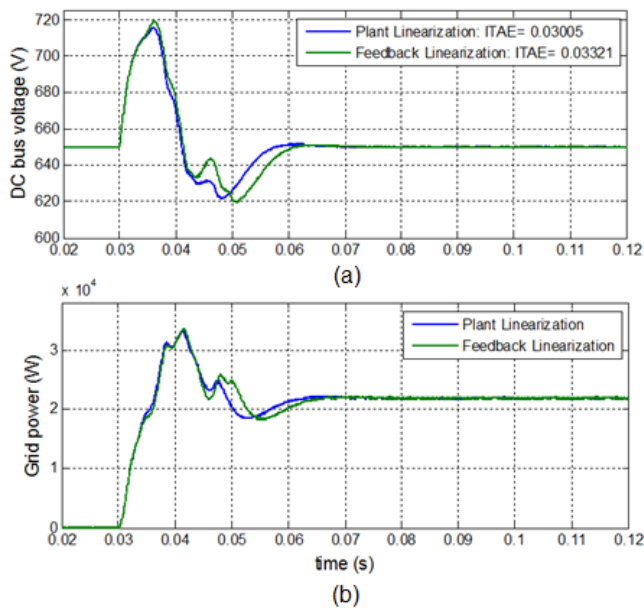


**Fig.10.** Transien Responses of the large disturbance (22000W power change): (a) the DC bus voltage (b) the active grid power

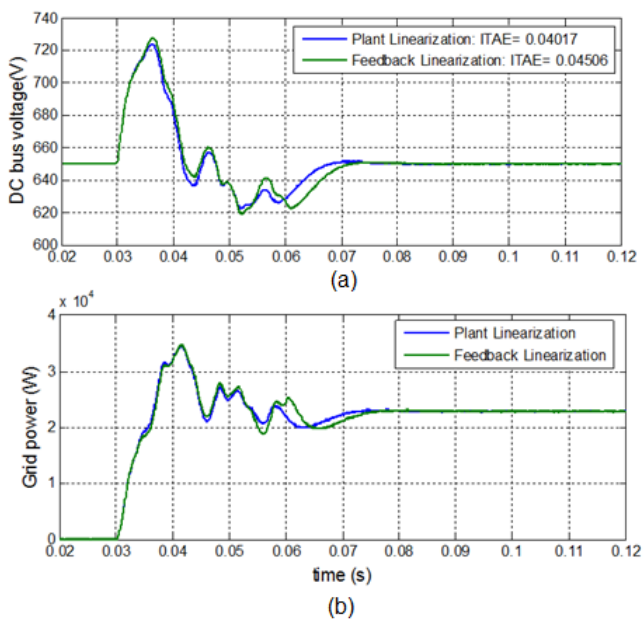


**Fig.11.** Transien Responses of the large disturbance (23000W power change): (a) the DC bus voltage (b) the active grid power

## 5. Conclusion

The performance investigation of the DC bus voltage regulation-PI controller based on the plant linearization and the feedback linearization techniques in response to the power change generated by renewable energy source have been conducted in this study. From the simulation results, it is shown that the dynamic and the transient response of the DC bus voltage regulation due to the instantaneous small changes of the power are relatively the same both for the plant linearization based-PI controller and the feedback linearization based-PI controller. However for the

instantaneous changes of the input power with relatively large magnitude, the dynamic of the DC bus voltage regulation of the plant linearization based-PI controller and the feedback linearization based-PI controller are relatively different. Although not too significant, it could be seen that the response of the PI controller based on plant linearization is more superior than that of the PI controller based on feedback linearization both in the overshoot and ITAE.

## Acknowledgements

This research was supported by RPP-Universitas Diponegoro [1051-127/UN7.5.1/PG/2016]

## References

- [1] Debouza, Mahdi, et al. "Design and implementation of a robust state-feedback control law for a grid-connected doubly fed induction generator wind turbine." 5th IET International Conference on Renewable Power Generation (RPG) 2016, 2016 page 47 (6 .)
- [2] Ajabi-Farshbaf, Rahim, et al. "Modelling of a New Configuration for DFIGs Using T-type Converters and a Predictive Control Strategy in Wind Energy Conversion Systems." International Journal of Renewable Energy Research (IJRER) 6.3 (2016): 975-986.
- [3] Al-Quteimat, Alaa, Alessandro Roccaforte, and Uwe Schäfer. "Performance improvement of direct torque control for doubly fed induction generator with 12 sector methodology." Renewable Energy Research and Applications (ICRERA), 2016 IEEE International Conference on. IEEE, 2016.
- [4] Purnomo, Mauridhi Hery, Iwan Setiawan, and Ardyono Priyadi. "Computational Intelligence Based Regulation of the DC Bus in the On-grid Photovoltaic System." Proceedings of Second International Conference on Electrical Systems, Technology and Information 2015 (ICESTI 2015). Springer Singapore, 2016.
- [5] Ahmadi, N., et al. "Frequency-dependent modeling of grounding system in EMTF for lightning transient studies of grid-connected PV systems." Renewable Energy Research and Applications (ICRERA), 2015 International Conference on. IEEE, 2015.
- [6] Popavath, Mr Lakshman Naik, and K. Palanisamy. "A Dual Operation of PV-Statcom as Active Power Filter and Active Power Injector in Grid Tie Wind-PV System." International Journal Of Renewable Energy Research 5.4 (2015): 978-982.
- [7] Sugahara, Yu, and Takaharu Takeshita. "Reactive current control of a multi-DC-voltage Cascade STATCOM." Renewable Energy Research and Applications (ICRERA), 2015 International Conference on. IEEE, 2015.
- [8] Aissa, Oualid, et al. "Analysis, design and real-time implementation of shunt active power filter for power quality improvement based on predictive direct power control." Renewable Energy Research and Applications

- (ICRERA), 2016 IEEE International Conference on. IEEE, 2016.
- [9] Moon, Ji-Woo, et al. "Model predictive control with a reduced number of considered states in a modular multilevel converter for HVDC system." *IEEE Transactions on Power Delivery* 30.2 (2015): 608-617.
- [10] Li, Shuhui, et al. "Neural-network based vector control of VSC HVDC transmission systems." *Renewable Energy Research and Applications (ICRERA), 2015 International Conference on. IEEE, 2015.*
- [11] Tarisciotti, Luca, et al. "Modulated model predictive control for a three-phase active rectifier." *IEEE Transactions on Industry Applications* 51.2 (2015): 1610-1620.
- [12] VARMA, DILEEP KUMAR, and Y. P. Obulesh. "An Improved Synchronous Reference Frame Controller based Dynamic Voltage Restorer for Grid Connected Wind Energy System." *International Journal of Renewable Energy Research (IJRER)* 6.3 (2016): 880-888.
- [13] Pena, R., J. C. Clare, and G. M. Asher. "Doubly fed induction generator using back-to-back PWM converters and its application to variable-speed wind-energy generation." *IEE Proceedings-Electric Power Applications* 143.3 (1996): 231-241.
- [14] Gonzalo Abad, et al. "Doubly Fed Induction Machine: Modeling and Control for Wind Energy Generation" A John Wiley and Son Inc (2011).
- [15] Song, Hong-seok, and Kwanghee Nam. "Dual current control scheme for PWM converter under unbalanced input voltage conditions." *Industrial Electronics, IEEE Transactions on* 46, no. 5 (1999): 953-959.
- [16] Setiawan, Iwan, Ardyono Priyadi, and Mauridhi Hery Purnomo. "Control Strategy Based on Associative Memory Networks for a Grid-Side Converter in On-Grid Renewable Generation Systems Under Generalized Unbalanced Grid Voltage Conditions." *International Review of Electrical Engineering (IREE)* 11.2 (2016): 171-182.
- [17] Preitl, Stefan, et al. "Controller design methods for driving systems based on extensions of symmetrical optimum method with DC and BLDC Motor Applications." *IFAC Proceedings Volumes* 45.3 (2012): 264-269.
- [18] Setiawan, Iwan, et al. "Adaptive B-spline neural network-based vector control for a grid side converter in wind turbine-DFIG systems." *IEEE Transactions on Electrical and Electronic Engineering* 10.6 (2015): 674-682.
- [19] Bajracharya, Chandra, et al: "Understanding of tuning techniques of converter controllers for VSC-HVDC.", *Nordic Workshop on Power and Industrial Electronics (NORPIE/2008)*, Espoo, Finland. Helsinki University of Technology (2008).